The International Journal of Advanced Manufacturing Technology (2022) 119:4693–4712
https://doi.org/10.1007/s00170-021-08491-4

ORIGINAL ARTICLE

Comparison of flexural strength of parts fabricated by vacuum casting with different fillers and fused deposition modeling with different printing angles

Chil-Chyuan Kuo[1,2] · **Hsueh-An Liu**[1] · **Zhi-Ming Chang**[1] · **Cheng-You Yu**[1] · **Hong-Yi Lian**[1]

Received: 17 September 2021 / Accepted: 30 November 2021 / Published online: 13 January 2022
© The Author(s), under exclusive licence to Springer-Verlag London Ltd., part of Springer Nature 2021

Abstract

Vacuum casting (VC) is a promising technique used for the production of functional plastic parts due to its fast production of high-quality prototypes. However, the mechanical properties of the fabricated products are affected by the composition of the molding materials. Additive manufacturing (AM) is also widely applied for low-volume prototyping applications. However, the mechanical properties of the fabricated products are affected by both build directions and printing angles. To investigate the difference in flexural strength of parts between vacuum casting and fused deposition modeling, glass fiber (GF) and carbon fiber (CF) are added to the matrix materials of polyurethane (PU) for improving the flexural strength of the molded products and three different printing angles and two build directions were applied in AM process. It was found that the flexure strength of the specimen fabricated by VC is generally greater than that of the specimen fabricated by AM. The highest flexure strength of the specimen fabricated by VC is 141 MPa, whereas the highest flexure strength of the specimen fabricated by FDM is only 102.7 MPa. The addition of short GF to the PU will increase the flexural strength. The flexural strength can be increased by about 41% when the PU is added with 4 wt.% short GF. The flexural strength can be increased by about 4.8% when the PU is added with 1 wt.% long GF. In contrast to above results, the flexural strength will be reduced when the PU is added with more than 2 wt.% long GF. On the contrary, the flexural strength can not be improved when the short CF or long CF is added to the PU. Finally, the flexural strength of the plastic prototype made by VC technology is superior to that of the plastic prototype made by FDM since the mechanical properties of the plastic prototype made by the FDM are affected by the build direction and printing angle.

Keywords Vacuum casting · Polyurethane · Carbon fiber · Glass fiber · Silicone rubber mold · Flexural strength

1 Introduction

Rapid manufacturing technology (RMT) is a term that integrates additive manufacturing (AM) and rapid tooling (RT) technologies. AM is a technology for creating physical models directly from CAD models. The RT generally concerns the production of tooling using parts manufactured by AM. The RMT has gained importance in the research and development stage since it compresses the duration of time-to-market of a new product. In general, integration of silicone rubber mold (SRM) and vacuum casting technology (VCT) [1] is widely used for rapid manufacturing prototypes since the SRM has flexible and elastic distinct features so that prototype with sophisticated geometries can be fabricated easily. Puerta et al. [2] proposed a new approach to determine the suitability of the use of standard tensile test specimens fabricated by both fused deposition modeling (FDM) and VCT. It was found that the surface quality of the model used for the creation of the SRM is an important issue in the VCT. Thian et al. [3] employed the VCT to manufacture gear with microstructure via the SRM via conventional vacuum casting process. The

✉ Chil-Chyuan Kuo
jacksonk@mail.mcut.edu.tw

[1] Department of Mechanical Engineering, Ming Chi University of Technology, No. 84, Gungjuan Road, 24301 New Taipei City, Taiwan

[2] Research Center for Intelligent Medical Devices, Ming Chi University of Technology, No. 84, Gungjuan Road, 24301 New Taipei City, Taiwan

major disadvantage of the conventional vacuum casting process is insufficient filling pressure and filling speed. Zhao et al. [4] replicated shark skin surface accurately in the large area to overcome some difficulties in the replication process using VCT. Results revealed that the process parameters played an important part to eliminate air-bubbles on the surface of the resin parts. Zhang and Hu [5] proposed the differential pressure technology to improve the quality of resin parts using VCT via the optimization method. The artificial fish-swarm algorithm was proved to optimize the response surface model of the warpage via the optimized process parameters. Kai et al. [6] integrated AM and RT as well as VCT for connectors. Results showed that a stereolithography apparatus (SLA) mold cannot be used directly in the vacuum casting process since the SLA mold must be broken into pieces for extracting the molded parts.

Xu et al. [7] fabricated of micro-groove on the surface of carbon fiber-reinforced plastic (CFRP) to enhance the connection strength of composite parts. Results showed that the micro-groove array structures on the CFRP surface can improve the tensile strength of the connection interface in the composite parts effectively. The tensile strength of the composite part with micro-grooves was increased by 80.93% compared with the composite part without micro-grooves. Hornig et al. [8] investigated the possibility of adjusting the interface between the integrated actuator and sensor layers to the epoxy based carbon fiber (CF) reinforced plastic laminates. It was found that it is possible to enhance the mechanical properties, especially the interlaminar energy release rate by using multilayered sensor–actuator layers with polyimide outer layers and layers with low shear stiffness in between. Yu et al. [9] investigated the effect of a thin carbon fiber coat on the durability of the carbon–glass hybrid fiber reinforced polymer bars in water. It was found that the diffusivity coefficient of the carbon fiber coat is higher than that of internal glass fiber reinforced plastics (GFRP) in the water. In addition, the HFRP bars have a higher diffusivity coefficient and saturation water absorption compared to the carbon–glass hybrid fiber reinforced polymer bars in water. Rochardjo and Budiyantoro [10] overmolded pretensioned unidirectional carbon fiber by polyamide contained 30 wt. % glass fiber (GF). Results showed that the optimum molding parameters are melting temperature of 278 °C and injection pressure of 122 bar, resulting in flexural strength of 248.6 MPa was obtained.

Epoxy resin [11], PU [12], or polyester [13] was widely used as the materials in the VCT. According to practical experiences, both RT and AM technologies are widely applied for low-volume prototyping applications. However, flexural strength of parts fabricated by pure polyurethane (PU) resin is not acceptable via vacuum casting. In addition, flexural strength of parts fabricated by FDM is affected by printing angles. To investigate the difference in flexural strength of parts between vacuum casting and fused deposition modeling, two reinforcing fillers, i.e., glass fiber (GF) and carbon fiber (CF) were added in PU resin. Three different printing angles and two build directions were applied in the AM process.

2 Experiment

Figure 1 shows the research process of this study. Two different kinds of methods were used to make specimens for bending test. Figure 2 shows the computer-aided design (CAD) model and dimensions of the bending test specimen. The length, width, and height are 90 mm, 35 mm, and 10 mm, respectively. The first method is that the specimen is made with PU resins filled with different weights of GF (Formosa Plastics Inc.) and CF (Formosa Plastics Inc.) using VCT to investigate the flexural strength since GF and CF are used as reinforcement in plastics industry since the mid-seventies. The length of long CF and long GF is about 25 mm. The length of short CF and short GF is about 5 mm. A room temperature vulcanization liquid silicone rubber (KE-1310ST, Shin Etsu Inc.) was selected as matrix materials to fabricate SRM for vacuum casting. The silicone rubber and curing agent (CAT-1310S, Shin Etsu Inc.) and were mixed in a weight ratio of 10:1. To reduce human error, a user-friendly man–machine interface was developed using a Visual Basic program to determine the amounts of both liquid silicone rubber and hardener. A vacuum machine (F-600, Feiling Inc.) was employed to remove air-bubbles resulting from the mixing process under vacuum conditions.

To understand the locations of both weld lines and air traps, the molding simulation software named Moldex 3D (R14 SP3OR, CoreTech System Inc.) was employed to analyze the filling process of the molding material. A vacuum casting machine was also used for generating a vacuum environment in both mixing chamber and casting chamber using a vacuum pump (V-VC 75, Gardner Denver Inc.). In general, the VCT involves five distinct stages, including preliminary, vacuuming, casting, vacuum relief, and post-processing stages. Figure 3 shows the five stages of the VCT. The P1, P2, and P3 represent the pressure of

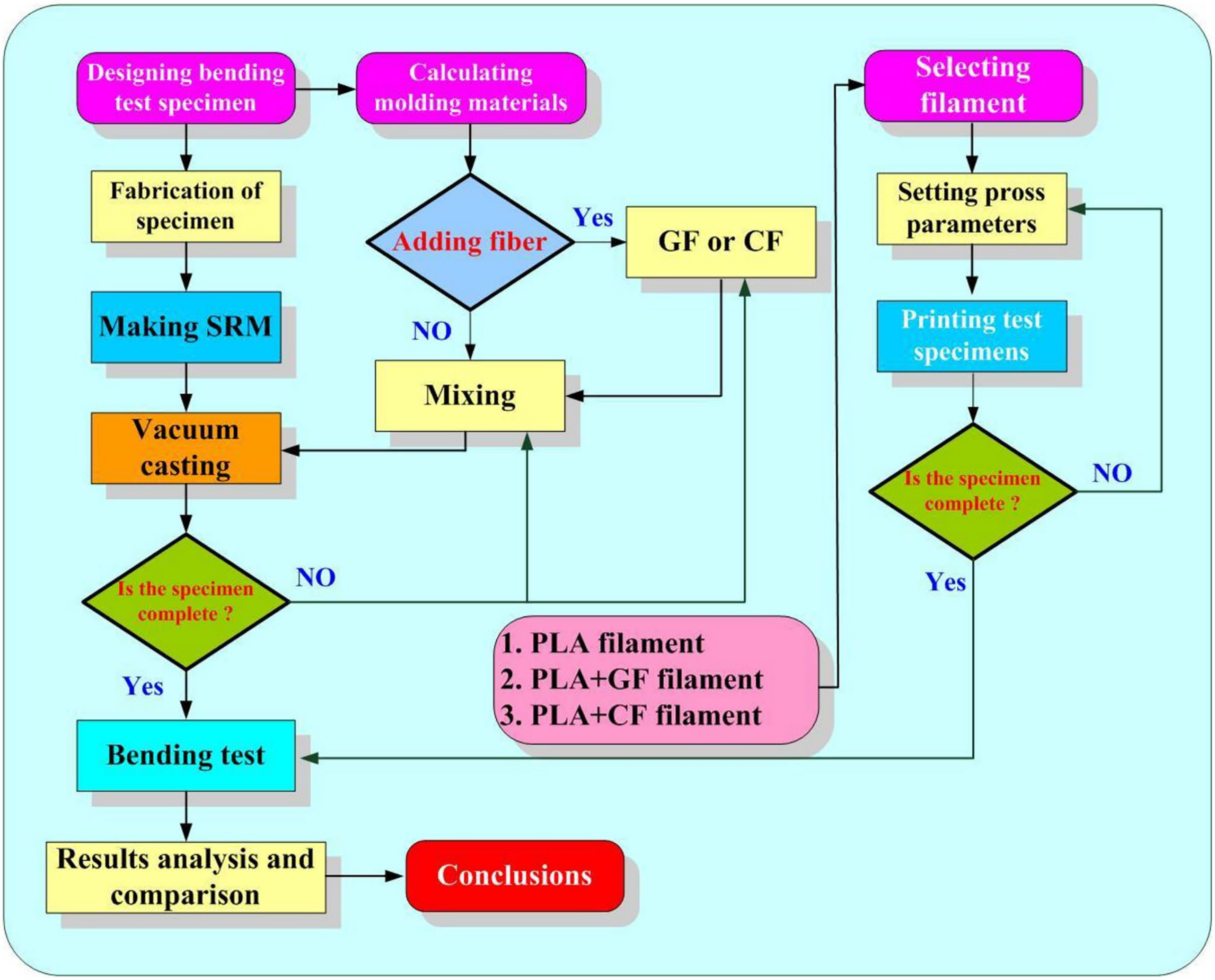
Designing bending test specimen
Calculating molding materials
Selecting filament
Fabrication of specimen
Adding fiber
Yes
GF or CF
Setting pross parameters
Making SRM
NO
Mixing
Printing test specimens
Vacuum casting
Is the specimen complete ?
NO
Is the specimen complete ?
NO
Yes
1. PLA filament
2. PLA+GF filament
3. PLA+CF filament
Yes
Bending test
Results analysis and comparison
Conclusions

Fig. 1 Research process of this study

mixing chamber, pressure of casting chamber, and atmospheric pressure, respectively. The preliminary stage is the preparation of SRM based on the size of the bending test specimen. The casting stage is the casting processing in the VC machine. The final stage is the post processing of molding parts. Figure 4 shows the schematic illustration of the manufacturing process of CF or GF added into the base materials of the PU resin to make bending test specimens.

Figure 5 shows the information regarding the ball value and intake area. The radii of ball valve, ball, and seat are 15 mm, 7.5 mm, and 6.25 mm, respectively. According to the law of cosines, the throughput of the ball valve can be calculated based on the following equation derived in this study. Figure 6 shows the throughput of the ball valve as a function of valve angle. In this study, the process parameters for producing bending test specimens include the SRM preheating temperature of 70 °C, stirrer speed of 600 rpm, molding material mixing time of 65 s, differential pressure time of 7 s, and ball valve angle of 60° [14].

$$\alpha = \cos^{-1}\left[\frac{(R\ \sin\ \theta)^2 + rBall^2 - rSeat^2}{2(R\ \sin\ \theta)(rBall)}\right] \tag{1}$$

$$\beta = \cos^{-1}\left[\frac{(R\ \sin\ \theta)^2 + rBall^2 - rSeat^2}{2(R\ \sin\ \theta)(rSeatl)}\right] \tag{2}$$

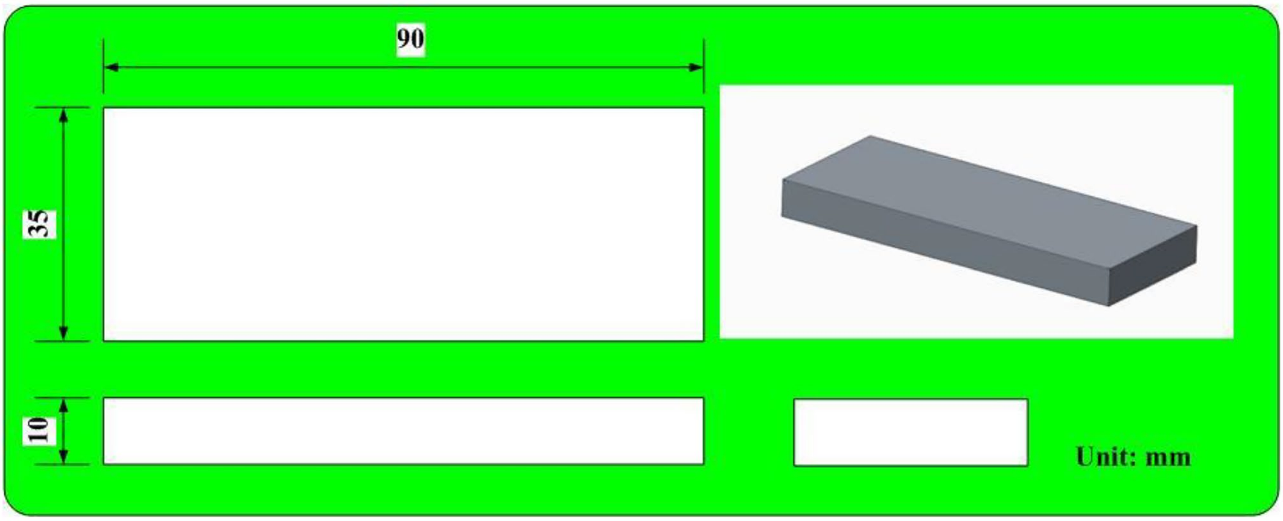
90
35
10
Unit: mm

Fig. 2 CAD model and dimensions of the bending test specimen

$$A = \left(\frac{2\alpha\pi rBall^2 + 2\beta\pi rseat^2}{360}\right) - (rBall^2\ \sin\ \alpha\ \cos\ \alpha + rSeat^2\ \sin\ \beta\ \cos\ \beta) \tag{3}$$

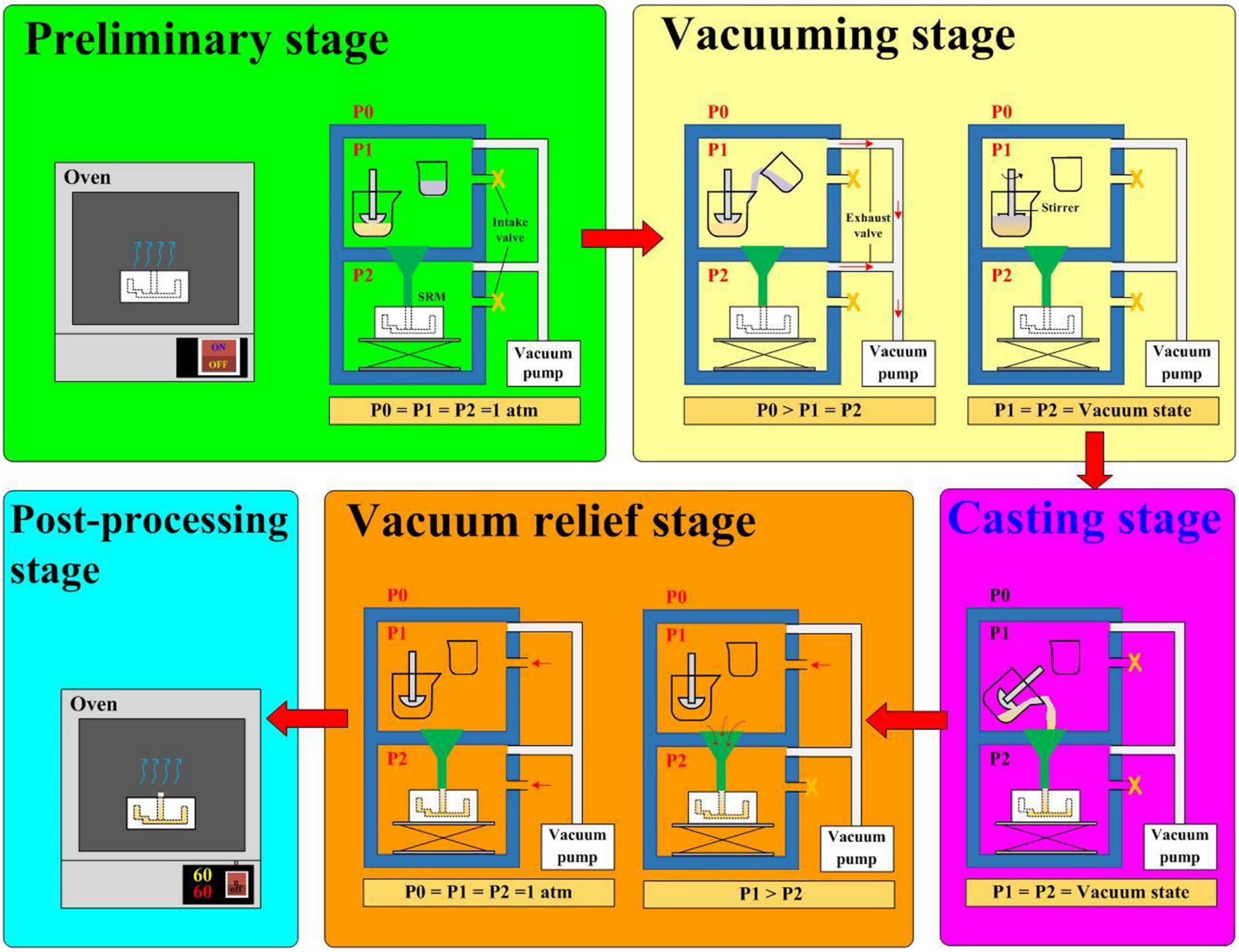
Preliminary stage
Oven
ON
OFF
P0
P1
P2
Intake valve
SRM
Vacuum pump
P0 = P1 = P2 =1 atm
Vacuuming stage
P0
P1
P2
Exhaust valve
Vacuum pump
P0 > P1 = P2
P0
P1
P2
Stirrer
Vacuum pump
P1 = P2 = Vacuum state
Casting stage
P0
P1
P2
Vacuum pump
P1 = P2 = Vacuum state
Vacuum relief stage
P0
P1
P2
Vacuum pump
P1 > P2
P0
P1
P2
Vacuum pump
P0 = P1 = P2 =1 atm
Post-processing stage
Oven
60
60

Fig. 3 Five stages of the VCT

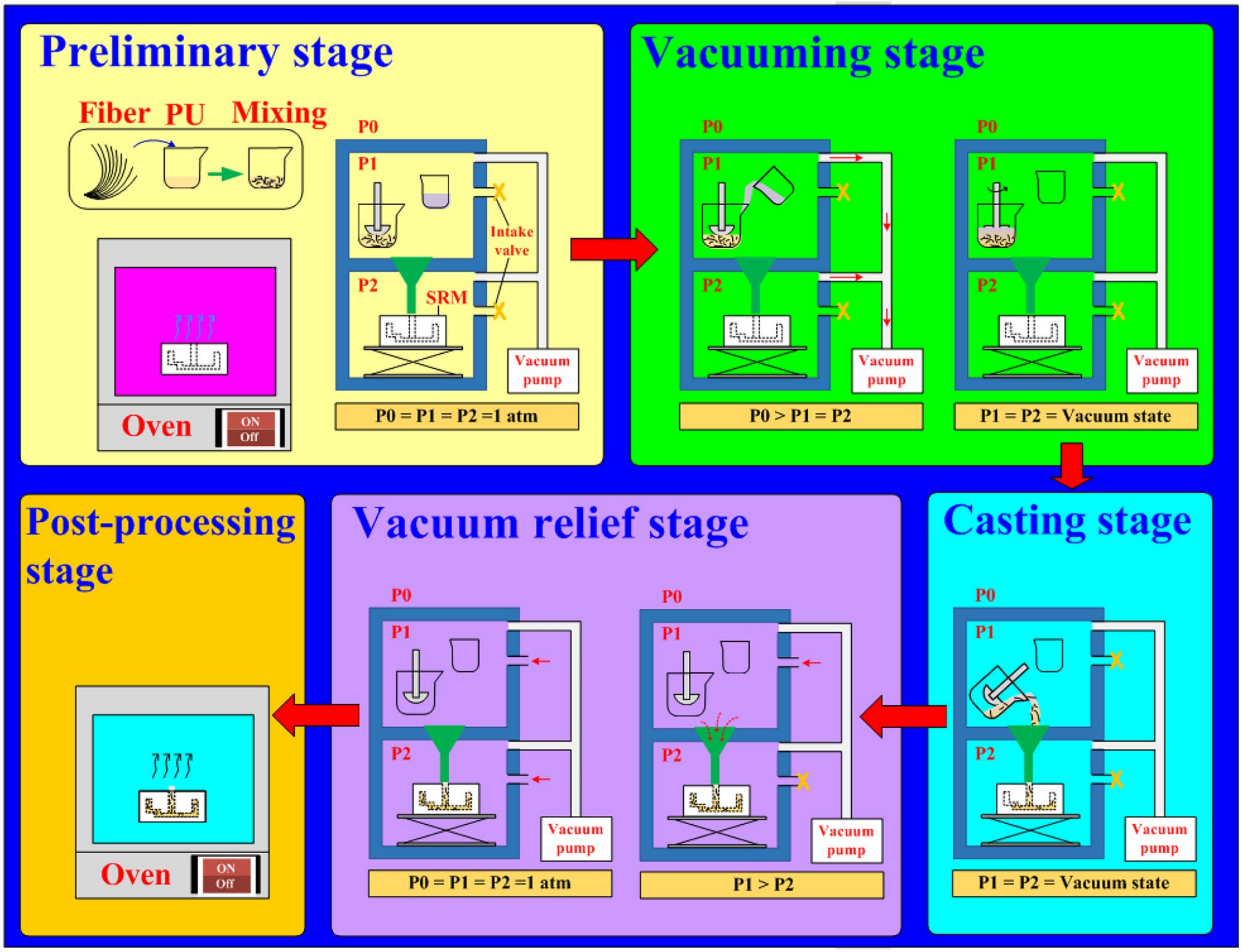
Preliminary stage
Fiber PU Mixing
P0
P1
Intake valve
P2
SRM
Vacuum pump
P0 = P1 = P2 =1 atm
Oven
ON
Off
Vacuuming stage
P0 > P1 = P2
P1 = P2 = Vacuum state
Casting stage
P1 = P2 = Vacuum state
Vacuum relief stage
P1 > P2
P0 = P1 = P2 =1 atm
Post-processing stage
Oven
ON
Off

Fig. 4 Schematic illustration of the manufacturing process of CF or GF added into the base materials of the PU resin to make bending test specimens

$$Q = \frac{v}{4}A\left(P_1 - P_0\right) = \frac{\sqrt{\frac{8kT}{\pi m}}}{4}A\left(P_1 - P_0\right) \tag{4}$$

where *rBall* is the radius of ball valve, *rSeat* is the radius of ball seat, *A* is the intake area, *Q* is the throughput of the valve, *v* is the average molecular velocity, P_1 is the

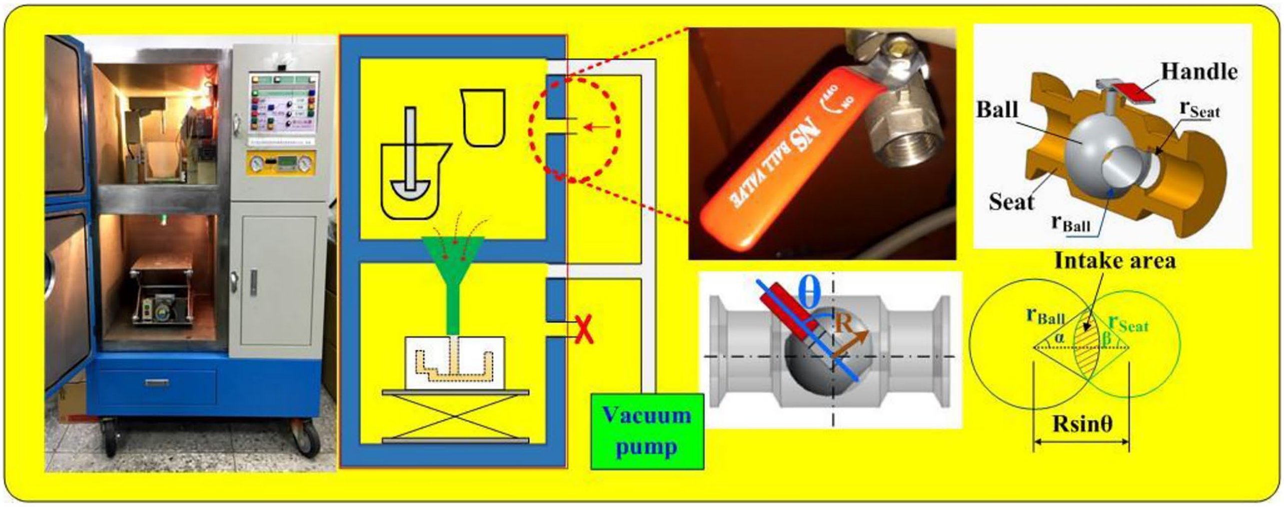
Vacuum pump
SN BALL VALVE
Handle
Ball
r_{Seat}
Seat
r_{Ball}
θ
R
Intake area
r_{Ball}
r_{Seat}
α
β
Rsinθ

Fig. 5 Information regarding the ball value and intake area

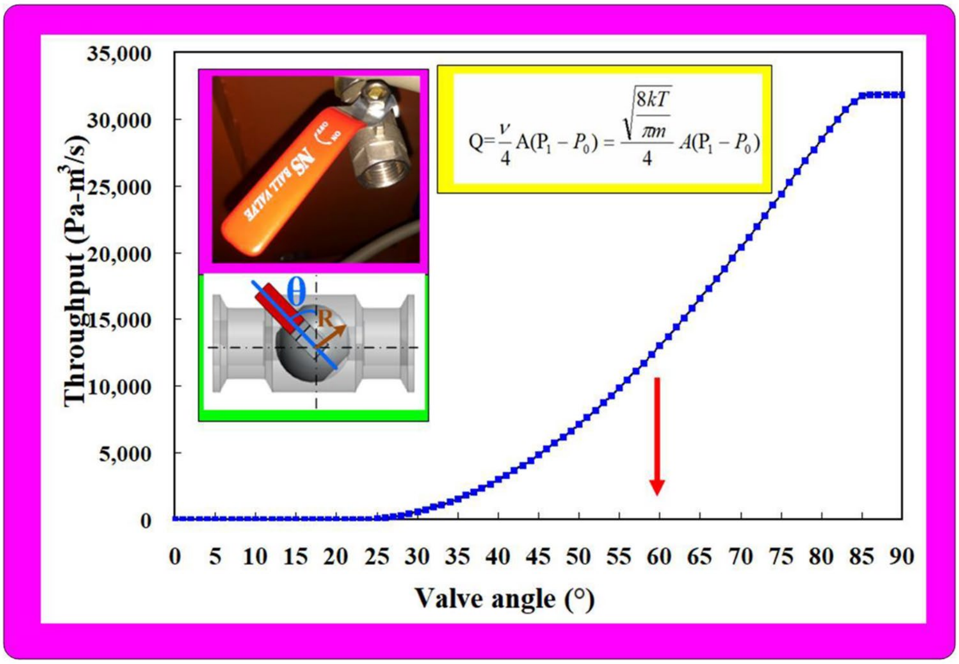

Fig. 6 Throughput of the ball valve as a function of valve angle

atmospheric pressure, P_0 is the terminal pressure, k is the Knudsen number [15], m is the molecular weight of gas, and T is the absolute temperature of 25 ℃. In this study, the PU resin was selected as molding materials. The base compound (UP-4290 N POLYOL, Sika AG Inc.) and hardener (UP-4290 N ISOCYANATE, Sika AG Inc.) were mixed in a weight ratio of 1:2.

The second method is that three kinds of PLA filaments, i.e., virgin PLA (Thunder 3D Inc.), PLA filled 10 wt.% GF (Thunder 3D Inc.) and 10 wt.% CF (Thunder 3D Inc.) are used to fabricate bending test specimens under two types of build directions and three printing angles. Figure 7 shows six different types of manufacturing bending test specimens using an FDM machine (Infinity X1E, Photonier Inc.). Three different printing angles are 30°, 45°, and 90°. Two build directions are horizontal printing and vertical printing. Thus, six different types of test specimens can be built by FDM.

To investigate the difference in flexural strength of those parts between vacuum casting and fused deposition modeling, three-point bending test [16] were carried out. To characterize fracture surfaces, optical microscopy (Quick Vision 404, Mitutoyo) was used to investigate defects, such as microcracks or porosity. The movement speed of the bending test punch is about 0.2 mm/s. The distance between support points is 80 cm. The applied force required to destroy the test specimens can be determined by the three-point bending test. Thus, flexural strength [17] can be determined by the following equation. In this study, the length between two supports is 80 mm.

$$\sigma = \frac{3PL}{2bd^2} \tag{5}$$

where P is the axial load at the fracture point, L is the length between two supports, b is the width of the bending test specimen, and d is the thickness of the bending test specimen.

3 Results and discussion

The main purpose of using numerical simulation is to investigate the flow behavior of the molding material and predict the accurate locations of venting hole in the silicone rubber mold. Boundary layer mesh (BLM) is one of the most suitable mesh technologies for computer-aided engineering application of plastic injection molding. In this study, the BLM was used to ensure the accuracy of simulation results because it is suitable for simulation models with intricate geometries. Figure 8 shows the simulation results of the filling process. The filling process is smooth and the filling time of the cavity is about 40 s. Note that the most common defects, such as weld lines, air-traps or short shot were not observed in the specimens. This means the filling system designed

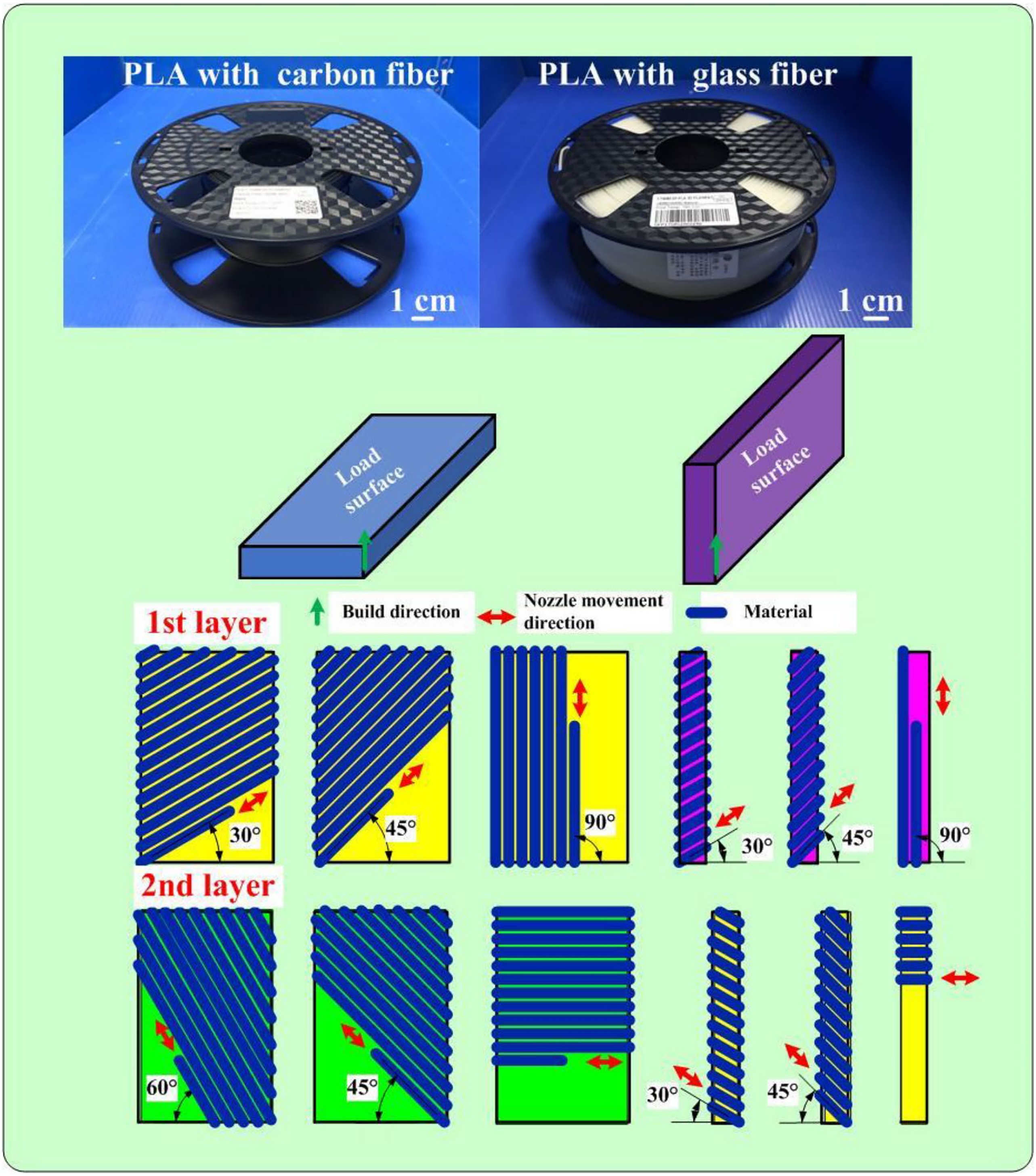
PLA with carbon fiber
PLA with glass fiber
1 cm
1 cm
Load surface
Load surface
1st layer
Build direction
Nozzle movement direction
Material
30°
45°
90°
30°
45°
90°
2nd layer
60°
45°
30°
45°

Fig. 7 Six different types of manufacturing bending test specimens using FFF

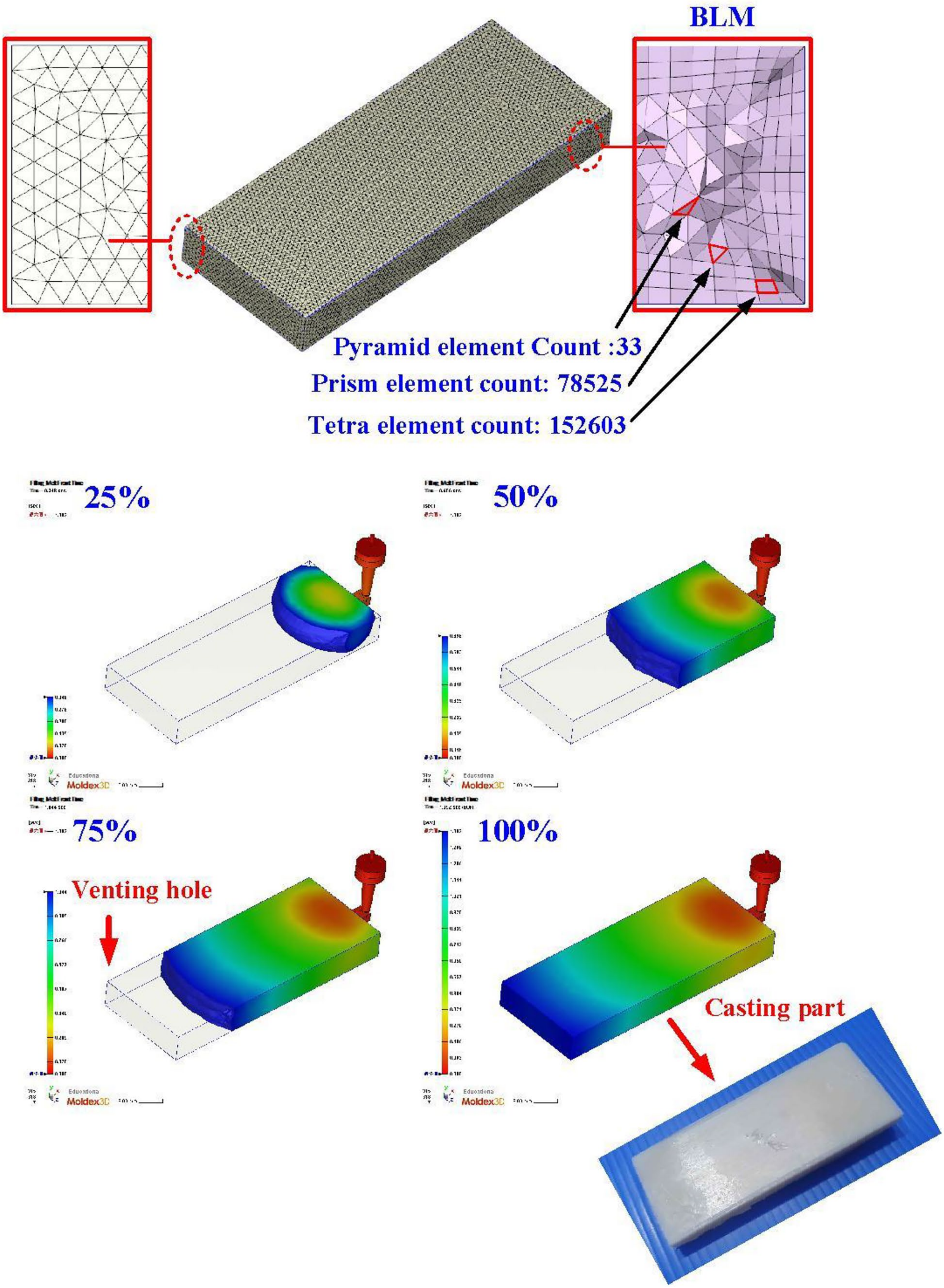
BLM
Pyramid element Count :33
Prism element count: 78525
Tetra element count: 152603
25%
50%
75%
100%
Venting hole
Casting part
Moldex3D
Moldex3D
Moldex3D
Moldex3D

Fig. 8 Simulation results of the filling process

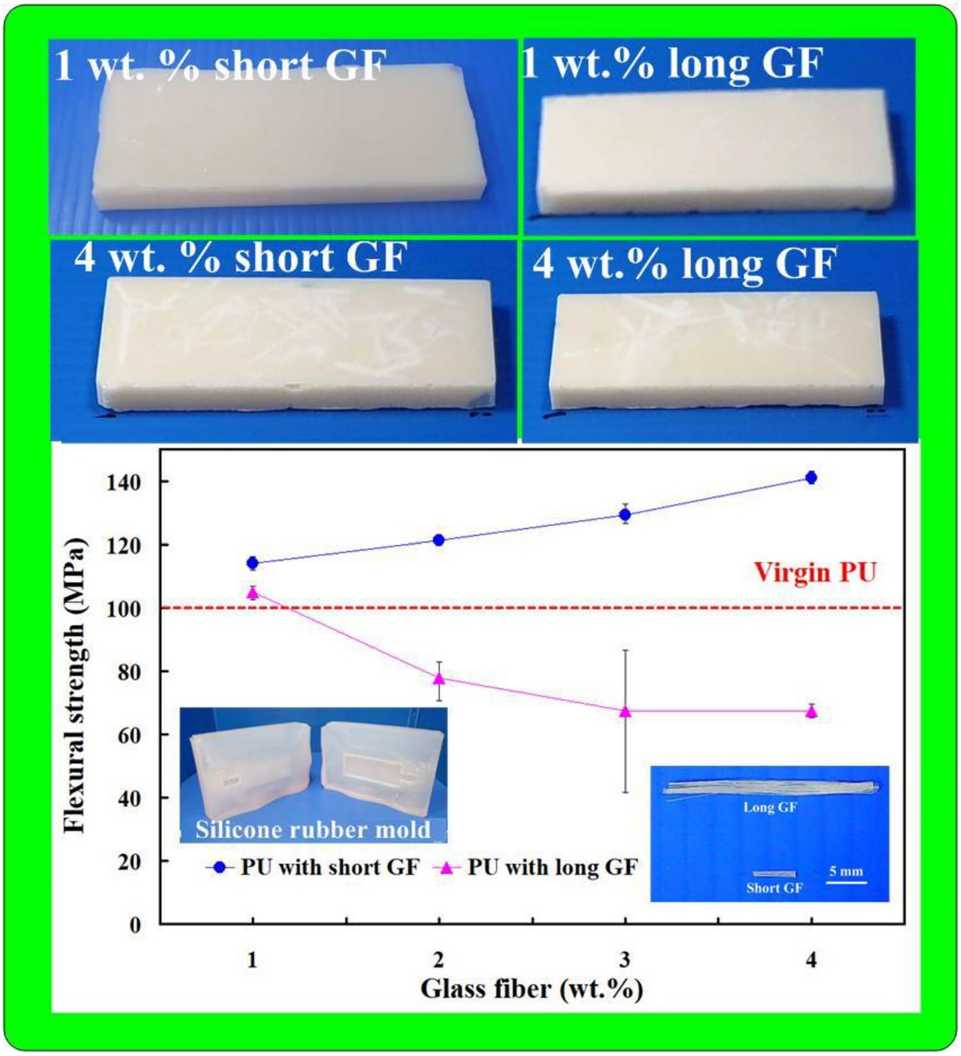

Fig. 9 Specimens fabricated by the PU filled with different weights of GF as a function of flexural strength

by this study has full contribution in the VC process. Figure 9 shows the specimens fabricated by the PU filled with different weights of GF as a function of flexural strength. Figure 10 shows the blending test situations of the specimens fabricated by the PU filled with different weights of short GF. The average flexural strength of the test specimen made with virgin PU is about 100 MPa. The average flexural strength of the test specimen fabricated by the PU filled with 1 wt.%, 2 wt.%, 3 wt.% and 4 wt.% short GF are about 114.1 MPa, 121.3 MPa, 129.3 MP, and 141 MPa, respectively. The average flexural strength of the test specimen fabricated by the PU filled with 1 wt.%, 2 wt.%, 3 wt.% and 4 wt.% long GF are about 105.1 MPa, 77.8 MPa, 67.4 MP, and 67.4 MPa, respectively. Three phenomena were found: (a) it is important to emphasize the fact that the PU added with short GF can increase the flexural strength. The flexural strength was enhanced by about 41% when the PU is added with 4 wt.% short GF, (b) the flexural strength was enhanced by about 4.8% when the PU is added with 1 wt.% long GF, and (c) the PU added with more than 2 wt.% of long GF can no longer increase the flexural strength due to the fluidity of the mixture is reduced, resulting in micro defeats in the test specimen. These defects include micro porosity [18] and microcracks [19]. Figure 11 shows the characterization of the fracture surfaces of the molded part fabricated by the PU filled with different weights of short GF and long GF.

Figure 12 shows the specimens fabricated by the PU filled with different weights of CF as a function of flexural strength. Figure 13 shows the blending test situations of the specimens fabricated by the PU filled

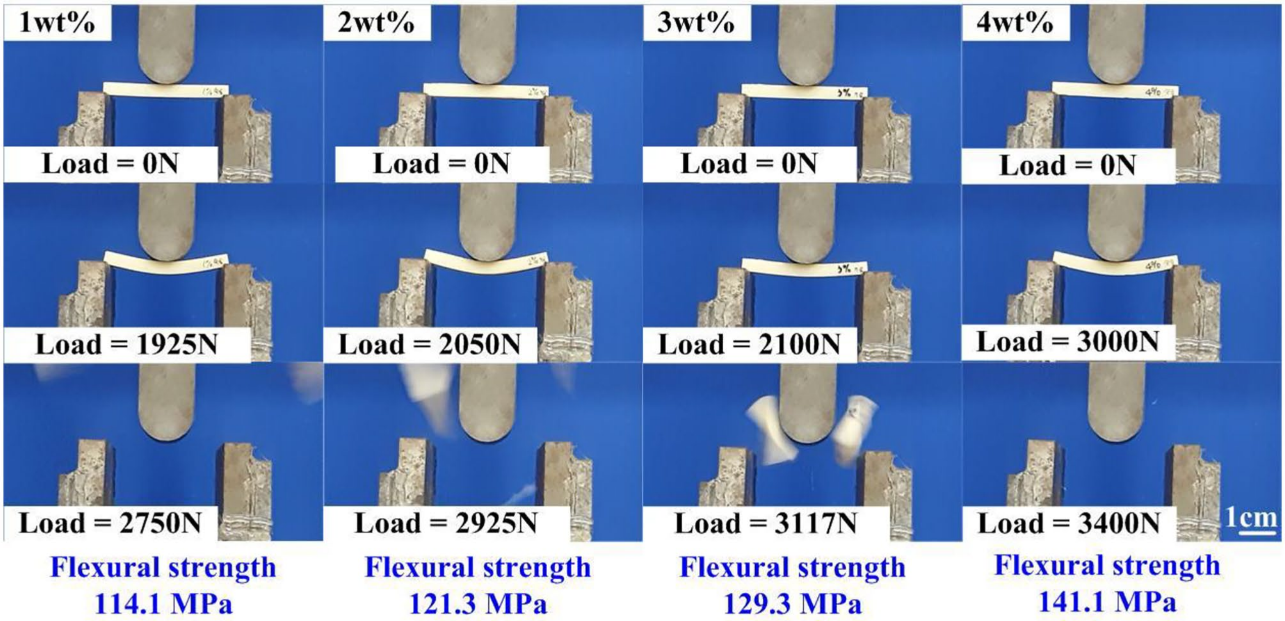
1wt%
2wt%
3wt%
4wt%
Load = 0N
Load = 0N
Load = 0N
Load = 0N
Load = 1925N
Load = 2050N
Load = 2100N
Load = 3000N
Load = 2750N
Load = 2925N
Load = 3117N
Load = 3400N
1cm
Flexural strength 114.1 MPa
Flexural strength 121.3 MPa
Flexural strength 129.3 MPa
Flexural strength 141.1 MPa

Fig. 10 Blending test situations of the specimens fabricated by the PU filled with different weights of short GF

with different weights of short CF. The average flexural strength of the test specimen fabricated by the PU filled with 1 wt.%, 2 wt.%, 3 wt.%, and 4 wt.% short CF is about 24.2 MPa, 22.5 MPa, 23.5 MP, and 24.2 MPa, respectively. The average flexural strength of the test specimen fabricated by the PU filled with 1 wt.%, 2

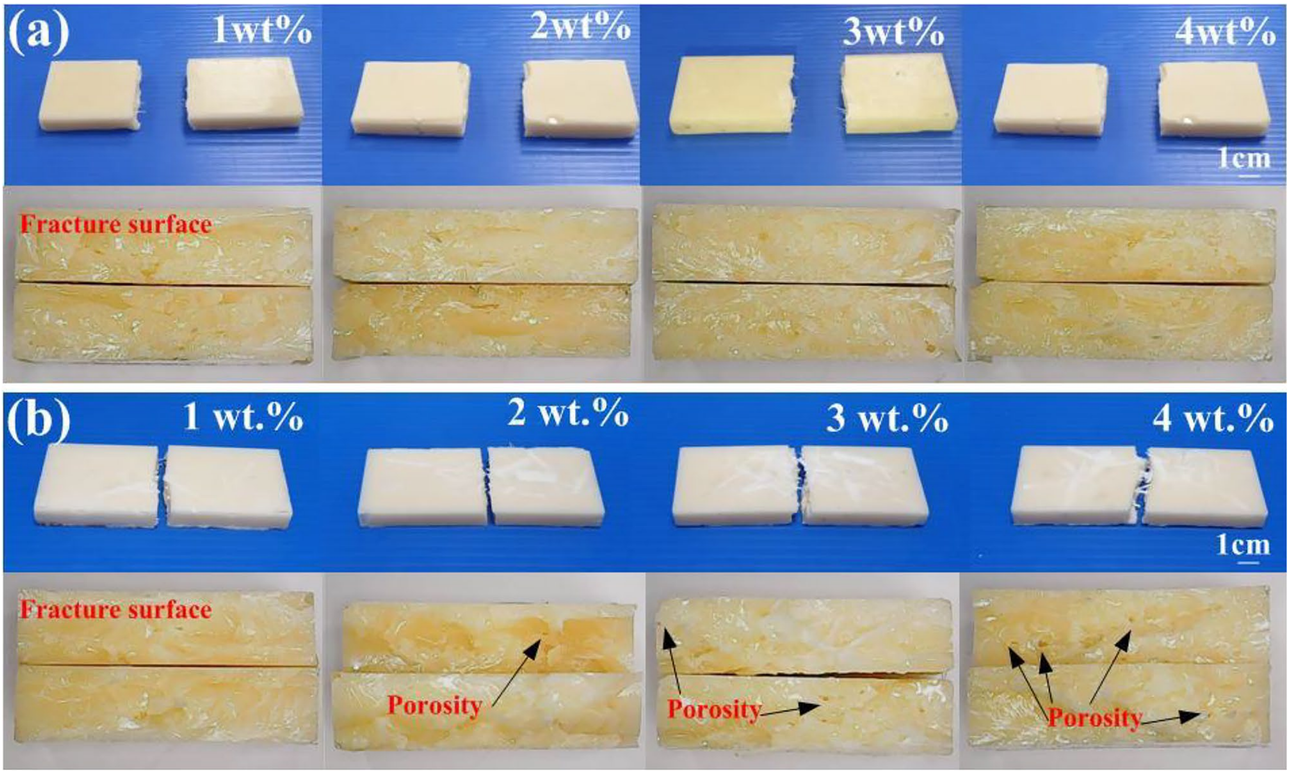
(a)
1wt%
2wt%
3wt%
4wt%
1cm
Fracture surface
(b)
1 wt.%
2 wt.%
3 wt.%
4 wt.%
1cm
Fracture surface
Porosity
Porosity
Porosity

Fig. 11 Characterization of the fracture surfaces of the molded part fabricated by the PU filled with different weights of a short GF and b long GF

Fig. 12 Specimens fabricated by the PU filled with different weights of CF as a function of flexural strength

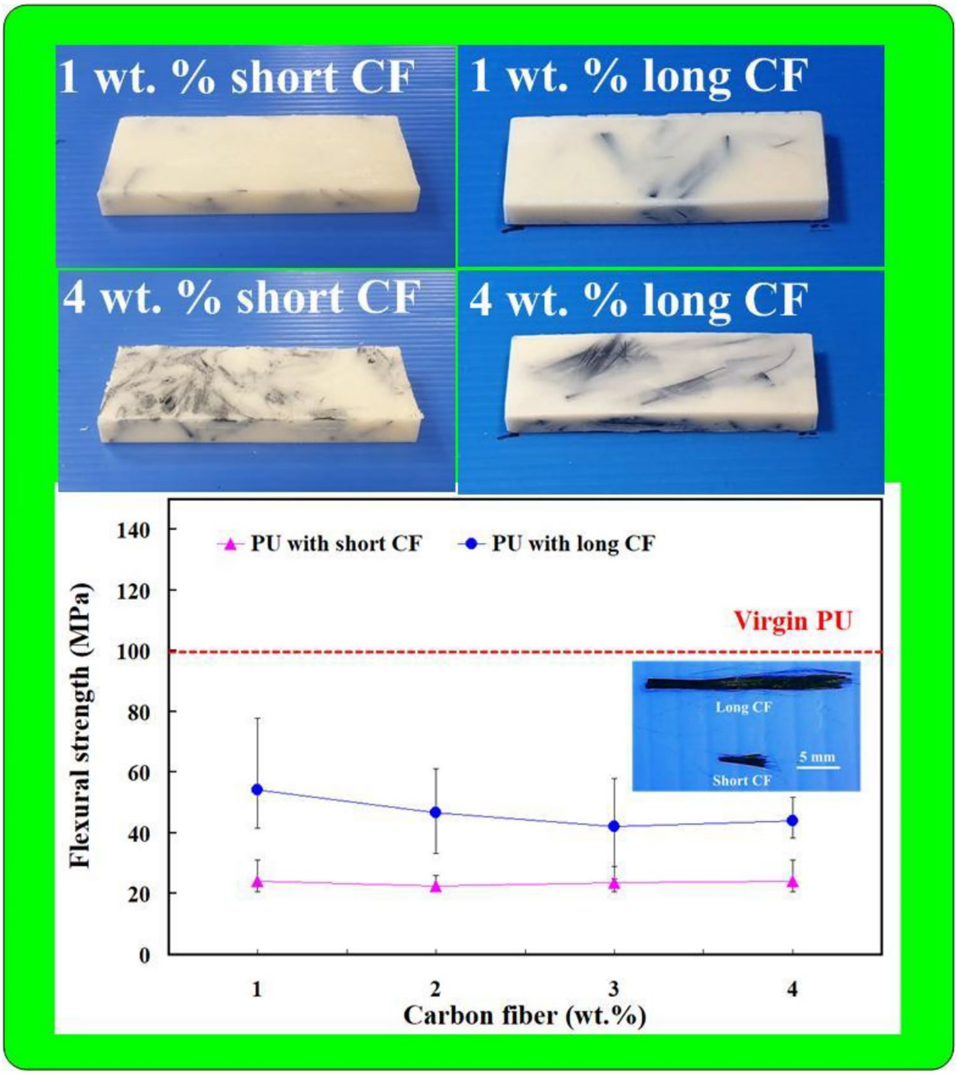

wt.%, 3 wt.%, and 4 wt.% long CF is about 54.3 MPa, 46.7 MPa, 42.2 MP, and 43.9 MPa, respectively. The flexural strength was reduced by about 75.9%, 77.6%, 76.6%, and 75.9% when the PU is added with 1 wt.%, 2 wt.%, 3 wt.%, and 4 wt.% of short CF, respectively. In addition, the flexural strength was reduced by about 45.9%, 53.5%, 57.9%, and 56.2% when the PU is added with 1 wt.%, 2 wt.%, 3 wt.%, and 4 wt.% of long CF, respectively. This means that short CF or long CF is not suitable for adding to the matrix materials of PU. The underlying reason probably could be attributed to the agglomeration [20] of CF in the fracture surface was found, since the CF can not result in chemical affinity [13] completely with PU. This hypothetical assumption was confirmed by the Fig. 14, showing the characterization of the fracture surfaces of the molded part fabricated by the PU filled with different weights of short CF and long CF. It was found that the flexural strength of the molded parts is not enhanced by adding short CF or long CF to the matrix materials of PU.

Figure 15 shows the specimens fabricated by the virgin PLA filament under different print angles as a function of flexural strength. Figure 16 shows the blending test situations of the specimens fabricated by the virgin PLA filament under different print angles. For the load direction is parallel to the build direction, the average flexural strength of the test specimens printed by printing angles of 30°, 45°, and 90° are approximately 32.9 MPa, 42.9 MPa, and 19 MPa, respectively. For the load direction is perpendicular to the build direction, the average flexural strength of the test specimens printed by printing angles of 30°, 45°, and 90°are approximately

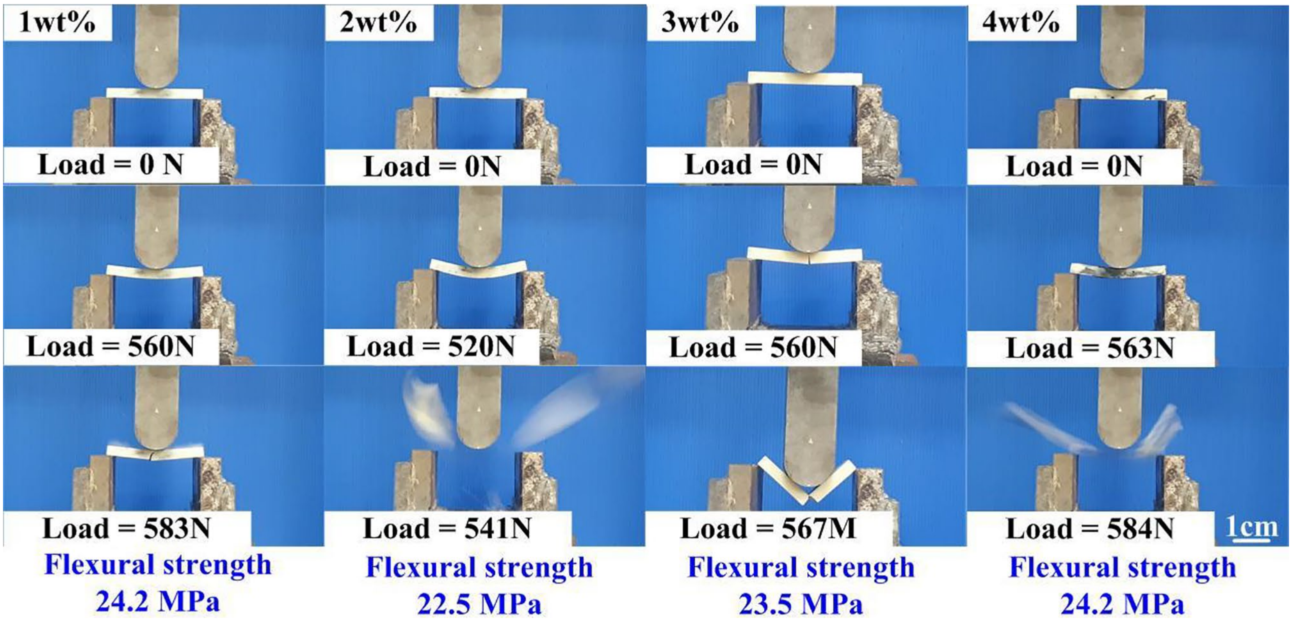
1wt%
2wt%
3wt%
4wt%
Load = 0 N
Load = 0N
Load = 0N
Load = 0N
Load = 560N
Load = 520N
Load = 560N
Load = 563N
Load = 583N
Load = 541N
Load = 567M
Load = 584N
1cm
Flexural strength 24.2 MPa
Flexural strength 22.5 MPa
Flexural strength 23.5 MPa
Flexural strength 24.2 MPa

Fig. 13 Blending test situations of the specimens fabricated by the PU filled with different weights of short CF

69.8 MPa, 81.9 MPa, and 58.4 MPa, respectively. Two phenomena were found. One is that the average flexural strength of the test specimen printed by the build direction perpendicular to the build direction is higher than those of the test specimens printed by the build direction parallel to the build direction. The other is that

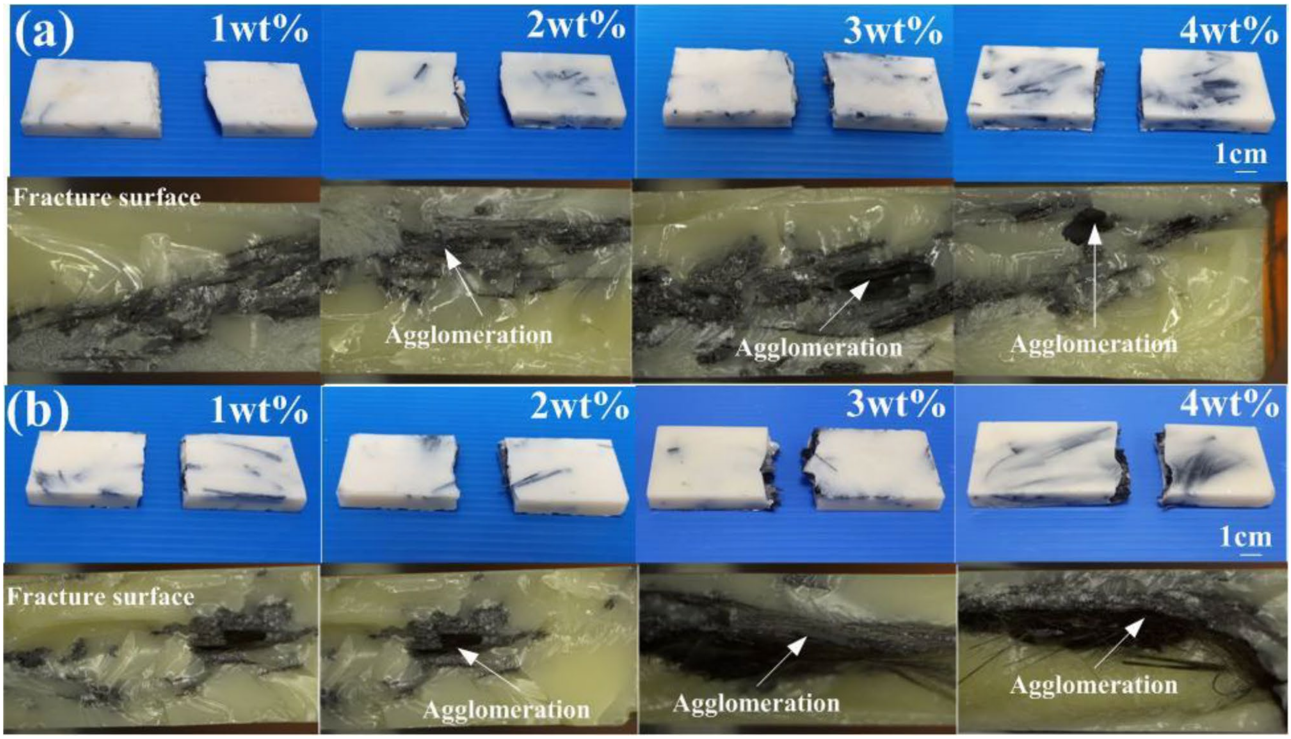
(a)
1wt%
2wt%
3wt%
4wt%
1cm
Fracture surface
Agglomeration
Agglomeration
Agglomeration
(b)
1wt%
2wt%
3wt%
4wt%
1cm
Fracture surface
Agglomeration
Agglomeration
Agglomeration

Fig. 14 Characterization of the fracture surfaces of the molded part fabricated by the PU filled with different weights of a short CF and b long CF

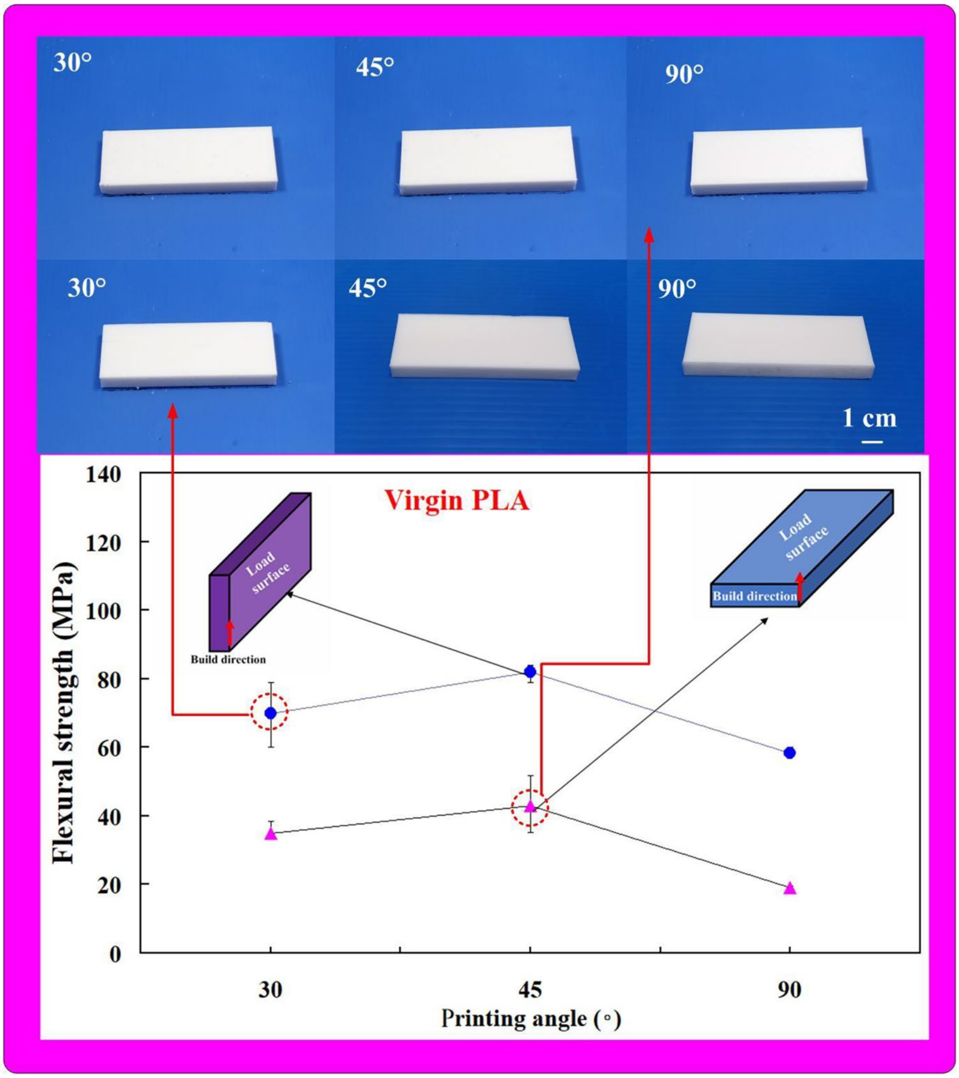

Fig. 15 Specimens fabricated by the virgin PLA filament under different print angles as a function of flexural strength

the average flexural strength of the printed test specimens printed by printing angles of 45° is higher than those of the printed test specimen printed by printing angles of 30° and 90°.

In general, specimens were stacked layer by layer during AM process. Figure 17 shows specimens fabricated by the PLA filled with GF filament under different print angles as a function of flexural strength. Figure 18 shows specimens fabricated by the PLA filled with CF filament under different print angles as a function of flexural strength. For the load direction is parallel to the build direction, the average flexural strength of the test specimens printed by printing angles of 30°, 45°, and 90° are approximately 74.3 MPa, 94.4 MPa, and 65.3 MPa, respectively. For the load direction is perpendicular to the build direction, the average flexural strength of the test specimens printed by printing angles of 30°, 45°, and 90°are approximately 91.9 MPa, 102.7 MPa, and 81.9 MPa, respectively. The results showed that similar results were found in the test specimens fabricated by the PLA filled with GF filament, showing the average flexural strength of the printed test specimens printed by printing angles of 45° was higher than those of the printed test specimens printed by printing angles of 30° and 90°, since the load direction is parallel to the direction of material stacking. In addition, the average flexural strength of the test specimens printed by the build direction perpendicular to the build direction is higher than those of the test specimens printed by the build direction parallel to the build direction.

Figure 19 shows the specimens fabricated by the PLA filled with CF filament under different print angles as a function of flexural strength. Figure 20 shows the bending test situations of the specimens fabricated by

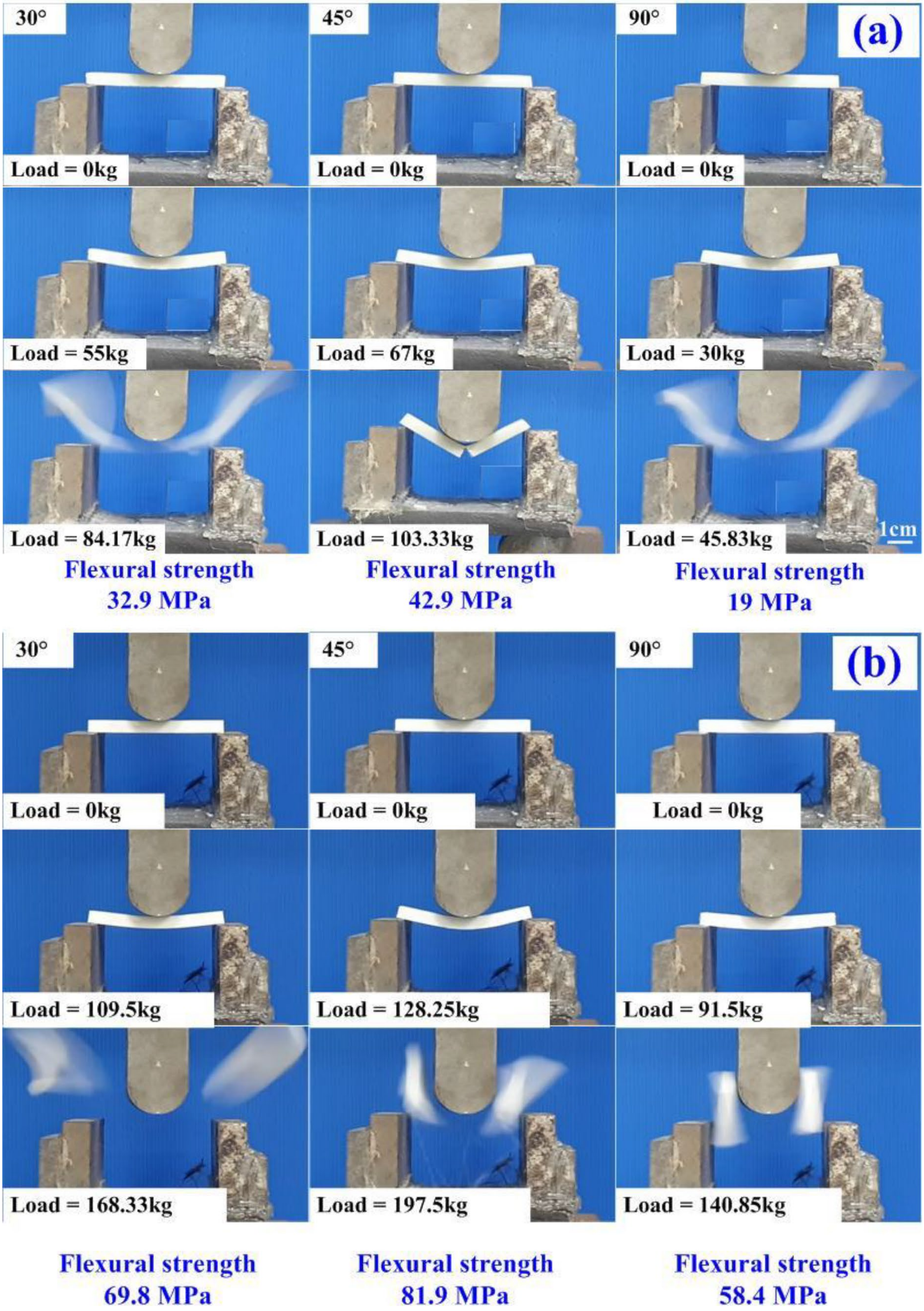
(a)
30°
45°
90°
Load = 0kg
Load = 0kg
Load = 0kg
Load = 55kg
Load = 67kg
Load = 30kg
Load = 84.17kg
Load = 103.33kg
Load = 45.83kg
1cm
Flexural strength 32.9 MPa
Flexural strength 42.9 MPa
Flexural strength 19 MPa
(b)
30°
45°
90°
Load = 0kg
Load = 0kg
Load = 0kg
Load = 109.5kg
Load = 128.25kg
Load = 91.5kg
Load = 168.33kg
Load = 197.5kg
Load = 140.85kg
Flexural strength 69.8 MPa
Flexural strength 81.9 MPa
Flexural strength 58.4 MPa

◀**Fig. 16** Blending test situations of the specimens fabricated by the virgin PLA filament under different print angles: (**a**) load direction is parallel to the build direction and (**b**) load direction is perpendicular to the build direction

the PLA filled with CF filament under different print angles. For the load direction is parallel to the build direction, the average flexural strength of the test specimens printed by printing angles of 30°, 45°, and 90° are approximately 47.7 MPa, 73.3 MPa, and 9.2 MPa, respectively. The average flexural strength of the test specimens printed by printing angles of 90° is the lowest becuase the load direction is parallel to the direction of material stacking. For the load direction is perpendicular to the build direction, the average flexural strength of the test specimens printed by printing angles of 30°, 45°, and 90°are approximately 78.1 MPa, 83.3 MP, and 79.2 MPa, respectively. The same results were found in the test specimens fabricated by the PLA filled with GF filament, showing the average flexural strength of the test specimens printed by the build direction perpendicular to the build direction is higher than those of the test specimens printed by the build direction parallel to the build direction. In addition, the average flexural strength of the printed test specimens printed by printing angles of 45° is higher than those of the printed test specimens printed by printing angles of 30° and 90°, since the load direction is parallel to the direction of material stacking. The highest flexure strength of the specimen fabricated by VC is 141 MPa. However, the highest flexure strength of the specimen fabricated by FDM is only 102.7 MPa. Based on the foregoing statements, it can be concluded that the flexural strength of the plastic prototype made by VCT is obviously better than that of the plastic prototype made by FDM, because the mechanical properties of the plastic prototype made by the FDM are impacted by both build direction [21] and printing angle [22] significantly.

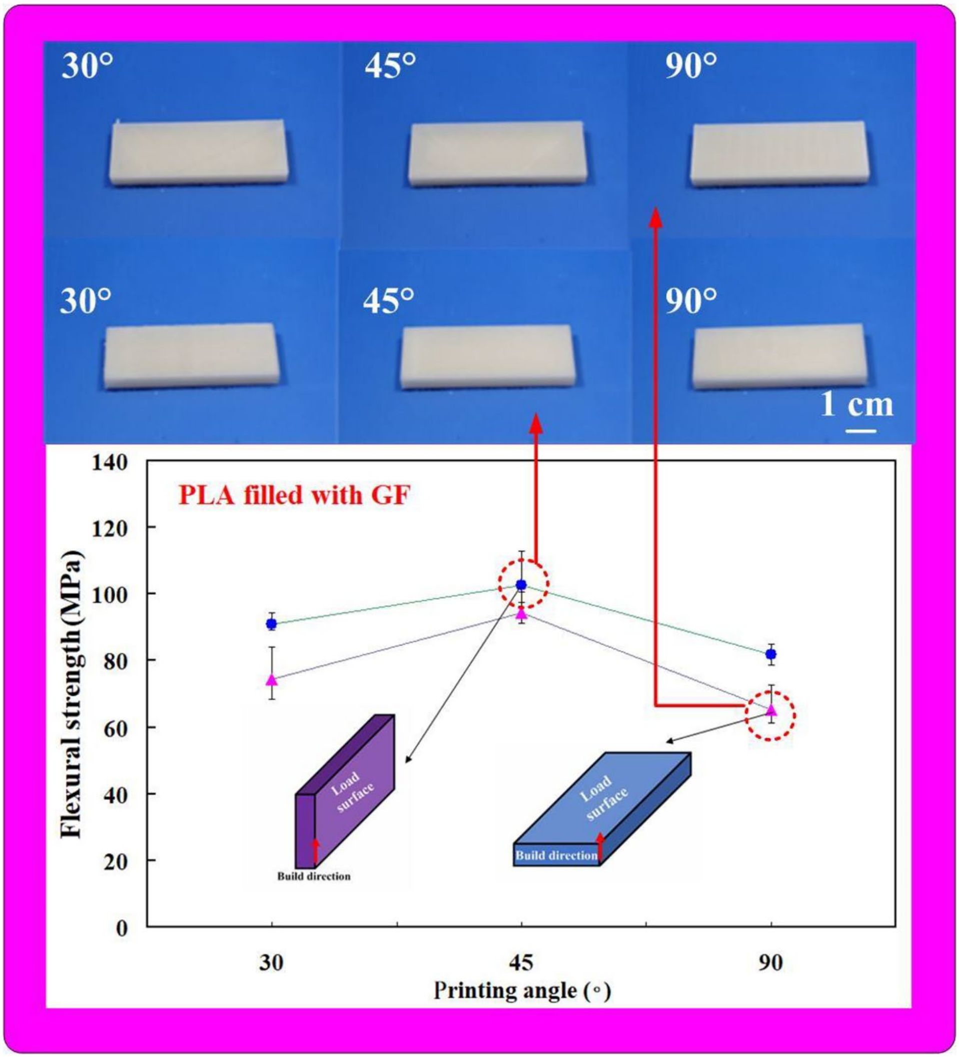

Fig. 17 Specimens fabricated by the PLA filled with GF filament under different print angles as a function of flexural strength

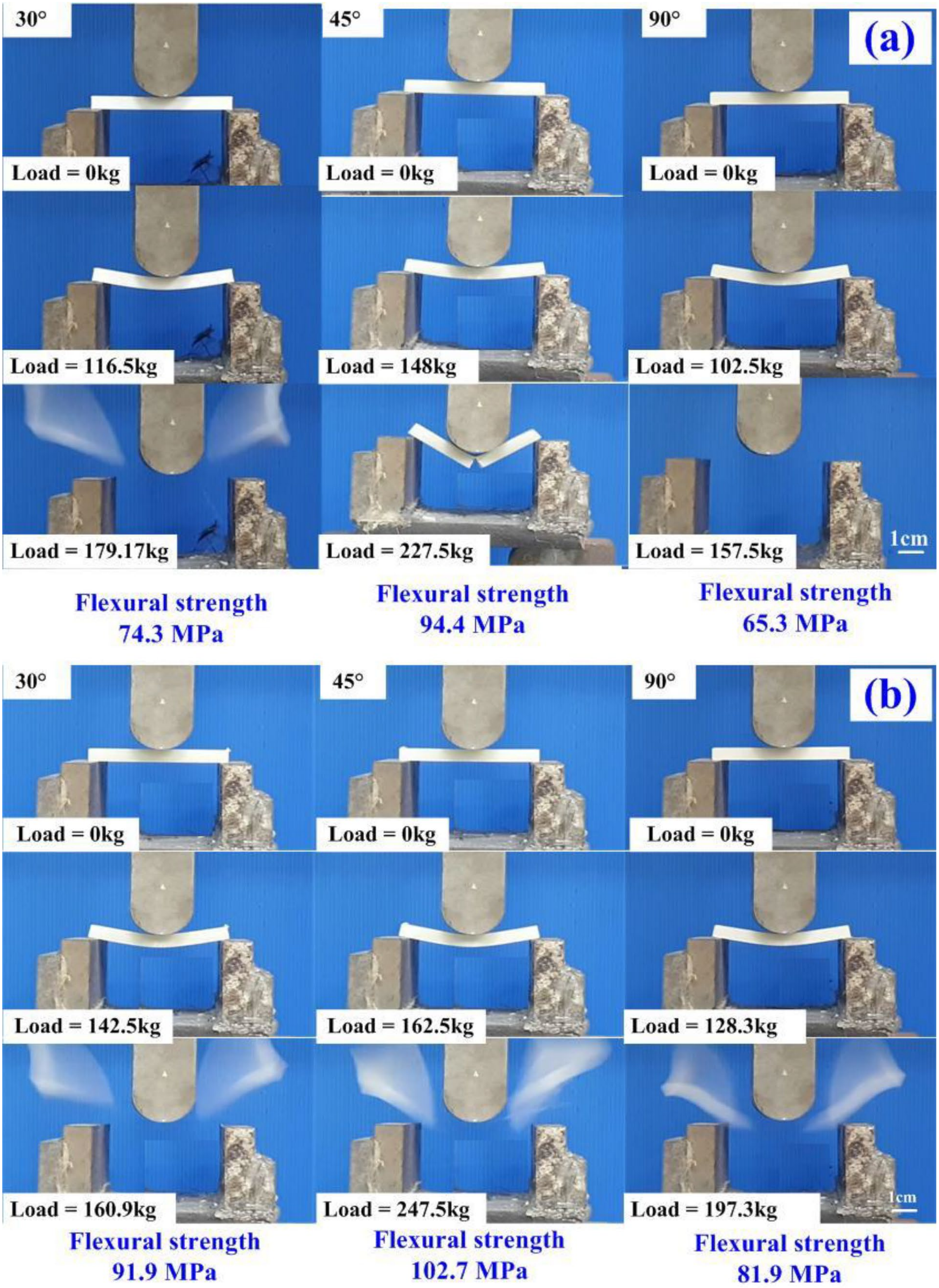
(a)
30°
Load = 0kg
Load = 116.5kg
Load = 179.17kg
Flexural strength 74.3 MPa
45°
Load = 0kg
Load = 148kg
Load = 227.5kg
Flexural strength 94.4 MPa
90°
Load = 0kg
Load = 102.5kg
Load = 157.5kg
1cm
Flexural strength 65.3 MPa
(b)
30°
Load = 0kg
Load = 142.5kg
Load = 160.9kg
Flexural strength 91.9 MPa
45°
Load = 0kg
Load = 162.5kg
Load = 247.5kg
Flexural strength 102.7 MPa
90°
Load = 0kg
Load = 128.3kg
Load = 197.3kg
1cm
Flexural strength 81.9 MPa

◂**Fig. 18** Blending test situations of the specimens fabricated by the PLA filled with GF filament under different print angles: (**a**) load direction is parallel to the build direction and (**b**) load direction is perpendicular to the build direction

According to those results of elaborate experiments, the findings in this study are very practical and provide potential applications of a new product during the research and development stage. The fabricated PU prototypes can further be processed, such as polishing, grinding, drilling, cutting, or tapping. Generally, temperature and pressure are the most significant variables in the VC process. To fulfill smart manufacturing for mass production while using VCT, both pressure and temperature sensors can be embedded in the cavity of SRM to record process parameters during the VC process. In this study, PU resin was used as molding materials. Other kinds of molding materials, such as epoxy resin, polycarbonate, nylon, acrylonitrile butadiene styrene, polypropylene, glass filled nylon, transparent polycarbonate, transparent acrylic, rubber and elastomers, and polyethylene can also be used to manufacture polymer prototypes. In this study, GF or CF was filled into PU to fabricate prototypes with high flexural strength. However, the mechanical properties of the test specimens fabricated by VCT are inferior to that fabricated by plastic injection molding because plastic injection molding is a high pressure manufacturing process [23]. Thus, the mechanical properties [24] of test specimen can further be improved by adding reinforcing fillers, such as bentonite, silsesquioxanes, silica, aluminum oxide, zirconia, silicon carbide, silicon nitride or molybdenum disulfide into the PU. These issues are currently being investigated and the results will be presented in a later study.

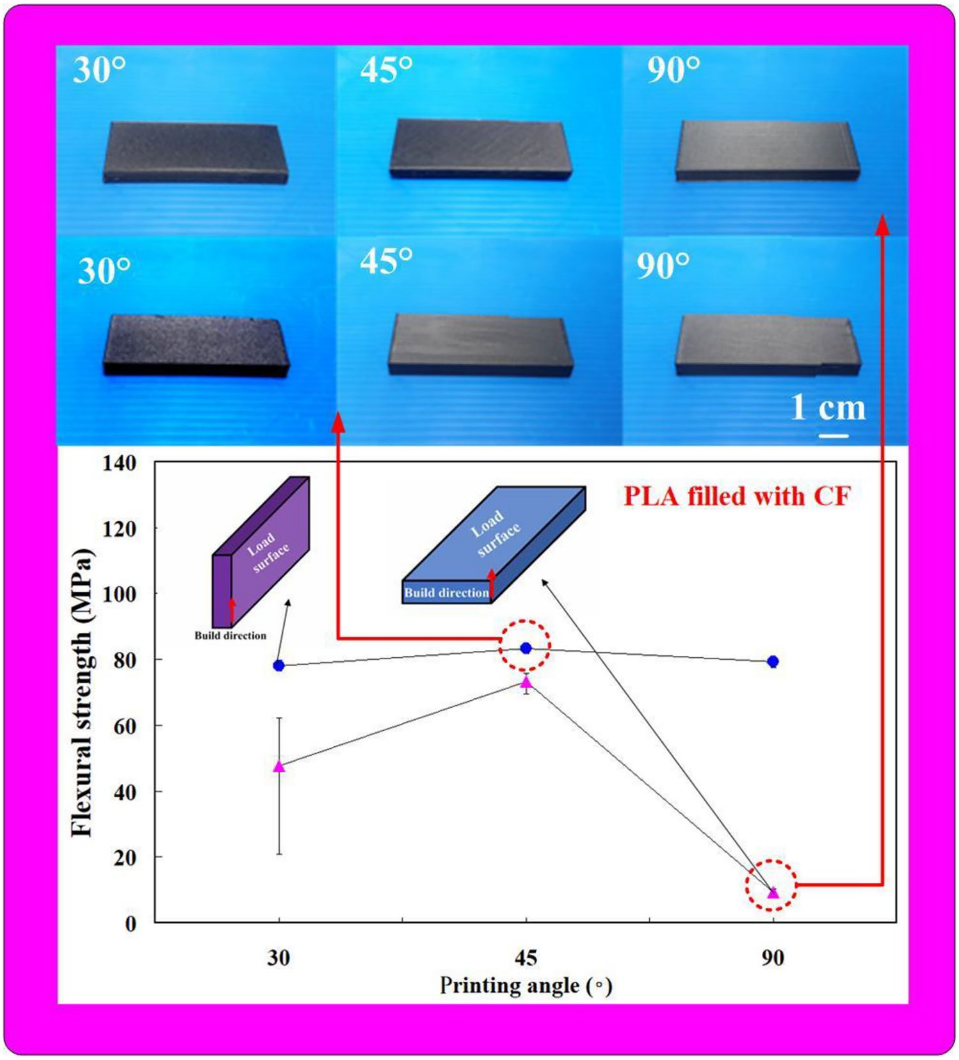

Fig. 19 Specimens fabricated by the PLA filled with CF filament under different print angles as a function of flexural strength

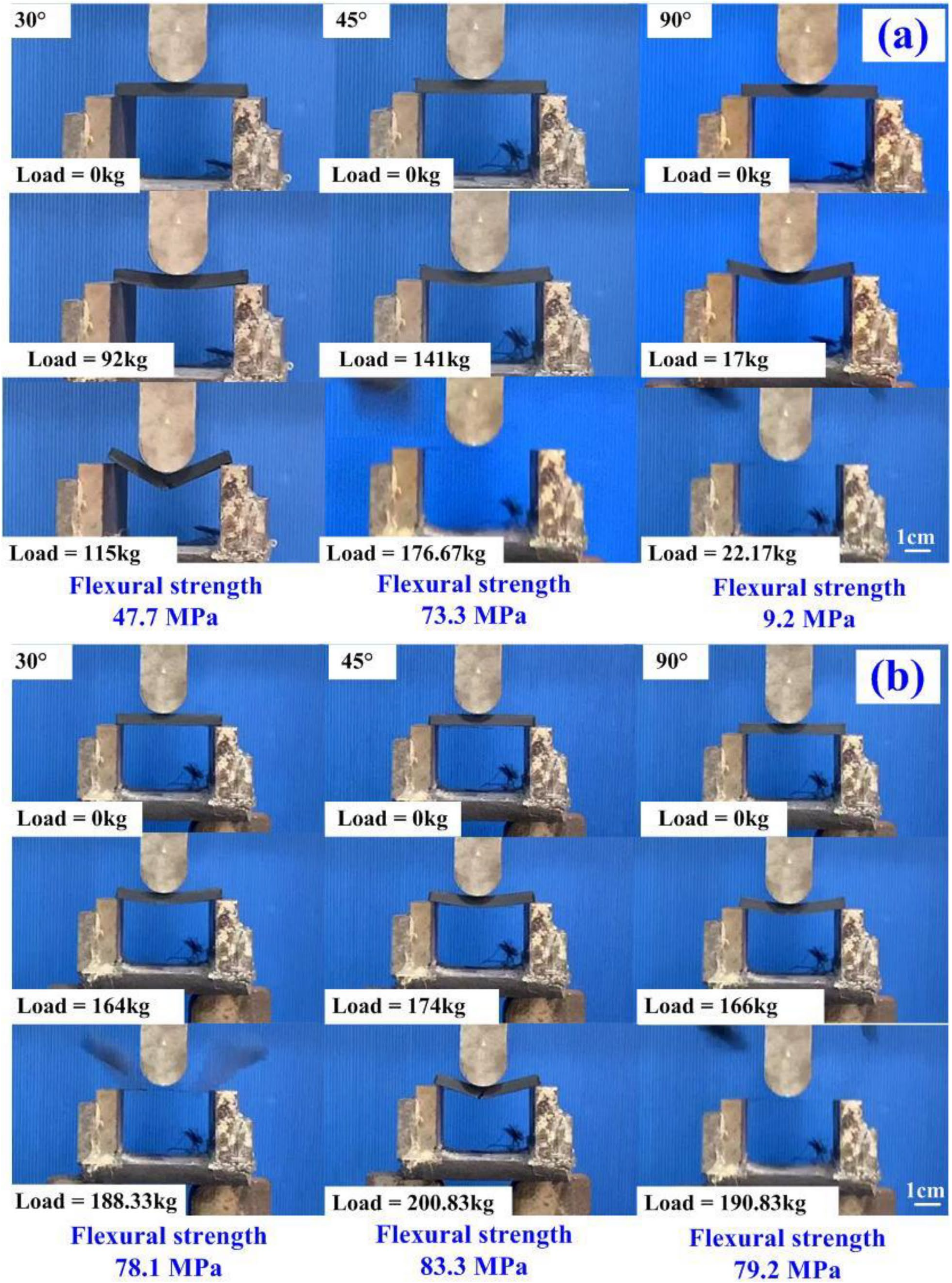
(a)
30°
Load = 0kg
Load = 92kg
Load = 115kg
Flexural strength 47.7 MPa
45°
Load = 0kg
Load = 141kg
Load = 176.67kg
Flexural strength 73.3 MPa
90°
Load = 0kg
Load = 17kg
Load = 22.17kg
Flexural strength 9.2 MPa
1cm
(b)
30°
Load = 0kg
Load = 164kg
Load = 188.33kg
Flexural strength 78.1 MPa
45°
Load = 0kg
Load = 174kg
Load = 200.83kg
Flexural strength 83.3 MPa
90°
Load = 0kg
Load = 166kg
Load = 190.83kg
Flexural strength 79.2 MPa
1cm

◀**Fig. 20** Blending test situations of the specimens fabricated by the PLA filled with CF filament under different print angles: (**a**) load direction is parallel to the build direction and (**b**) load direction is perpendicular to the build direction

4 Conclusions

It is well known that AM or VCT is frequently employed for the production of small series of plastic prototype. To investigate the difference in flexural strength of parts between VCT and AM, GF and CF were added to PU matrix materials for improving the flexural strength of the molded products and three different printing angles and two build directions were applied in AM process. The effects of two fibers added to the matrix material in different weight ratios on the flexural strength were investigated via bending test. In addition, CF or GF reinforced PLA filaments were employed to print plastic prototype via a FDM machine. The main conclusions from the experimental work in this study are as follows:

1. The flexure strength of the specimen fabricated by VC is generally greater than that of the specimen fabricated by AM because flexure strength of the specimen fabricated by AM is affected by both printing angle and build direction significantly. The highest flexure strength of the specimen fabricated by VC is 141 MPa, while the highest flexure strength of the specimen fabricated by FDM is only 102.7 MPa.
2. The addition of short GF to the PU will increase the flexural strength. The flexural strength can be increased by about 41% when the PU is added with 4 wt.% short GF. This material formula can be employed for low-volume production of prototypes for different industrial usages, such as prosthetics, automotive components medical devices, aerospace components, or consumer plastic components.
3. The flexural strength can be increased by about 4.8% once the PU is added with 1 wt.% long GF. However, the flexural strength will be reduced when the PU is added with more than 2 wt.% long GF due to the fluidity of the mixture is reduced, resulting in porosity and microcracks appeared in the test specimen.
4. The flexural strength can not be improved when the short CF or long CF is added to the PU since the CF and PU cannot produce chemical affinity after VC. In addition, the agglomeration of CF was found in the test specimen.

Author contribution Chil-Chyuan Kuo: wrote the paper, conceived and designed the analysis, performed the analysis/conceptualization. Hsueh-An Liu, Zhi-Ming Chang, Cheng-You Yu, Hong-Yi Lian: collected the data, contributed data or analysis tools.

Funding This study received financial support by the Ministry of Science and Technology of Taiwan under contract nos. MOST 110–2221-E-131–023 and MOST 109–2637-E-131–004.-

Declarations

Ethics approval Not applicable.

Conflict of interest The authors declare no competing interests.

References

1. Zhan SA, Song JT, Ding MH, Guo J, Liu HH (2017) A study of thin-walled ZL105A casting manufactured by vacuum differential pressure casting. Advanced in Engineering Research 135:574–582
2. Puerta APV, Sanchez DM, Batista M, Salguero J (2018) Criteria selection for a comparative study of functional performance of Fused Deposition Modelling and Vacuum Casting processes. J Manuf Process 35:721–727
3. Thian SCH, Tang Y, Tan WK, Fuh JYH, Wong YS, Loh HT, Lu L (2008) The manufacture of micromould and microparts by vacuum casting. Int J Adv Manuf Technol 38(9–10):944–948
4. Zhao DY, Huang ZP, Wang MJ, Wang T, Jin Y (2012) Vacuum casting replication of micro-riblets on shark skin for drag-reducing applications. J Mater Process Technol 212(1):198–202
5. Zhang HG, Hu QX (2016) Study of the filling mechanism and parameter optimization method for vacuum casting. Int J Adv Manuf Technol 83(5–8):711–720
6. Kai CC, Howe CT, Hoe EK (1998) Integrating rapid prototyping and tooling with vacuum casting for connectors. Int J Adv Manuf Technol 14:617–623
7. Xu B, Wei M-Y, Wu X-Y, Fu L-Y, Luo F, Lei J-G (2021) fabrication of micro-groove on the surface of CFRP to enhance the connection strength of composite part. Polymers 13:4039
8. Hornig A, Winkler A, Bauerfeind E, Gude M, Modler N (2021) Delamination behaviour of embedded polymeric sensor and actuator carrier layers in epoxy based CFRP laminates—a study of energy release rates. Polymers 13:3926
9. Yu Y, Pan Y, Zhou R, Miao X (2021) Effects of water and alkaline solution on durability of carbon-glass hybrid fiber reinforced polymer bars. Polymers 13:3844
10. Rochardjo HSB, Budiyantoro C (2021) Manufacturing and analysis of overmolded hybrid fiber polyamide 6 composite. Polymers 13:3820
11. Hong Y, Goh M (2021) Advances in liquid crystalline epoxy resins for high thermal conductivity. Polymers 13:1302
12. Chen G, Liu J, Zhang W, Han Y, Zhang D, Li J, Zhang S (2021) Lignin-based phenolic foam reinforced by poplar fiber and isocyanate-terminated polyurethane prepolymer. Polymers 13:1068
13. Nanaki SG, Christodoulou E, Bikiaris ND, Kapourani A, Kontogiannopoulos KN, Vergkizi-Nikolakaki S, Barmpalexis P (2021) Leflunomide sustained skin delivery based on sulfobetaine-modified chitosan nanoparticles embedded in biodegradable polyesters films. Polymers 13:960
14. Kuo CC, Liu HA, Chang CM (2020) Optimization of vacuum casting process parameters to enhance tensile strength of components using design of experiments approach. Int J Adv Manuf Technol 106:3775–3785
15. White J (2010) A gas lubrication equation for high Knudsen number flows and striated rough surfaces. J Tribol-Trans ASME 132(2):1–9
16. Ehrmann G, Ehrmann A (2021) Pressure orientation-dependent recovery of 3D-printed PLA objects with varying infill degree. Polymers 13:1275

17. Benkhelladi A, Laouici H, Bouchoucha A (2020) Tensile and flexural properties of polymer composites reinforced by flax, jute and sisal fibres. Int J Adv Manuf Technol 108:895–916
18. Dhavalikar P, Shenoi J, Salhadar K, Chwatko M, Rodriguez-Rivera G, Cheshire J, Foudazi R, Cosgriff-Hernandez E (2021) Engineering toolbox for systematic design of polyHIPE architecture. Polymers 13:1479
19. Dhimole VK, Serrao P, Cho C (2021) Review and suggestion of failure theories in voids scenario for VARTM processed composite materials. Polymers 13:969
20. Ramanavicius S, Jagminas A, Ramanavicius A (2021) Advances in molecularly imprinted polymers based affinity sensors (review). Polymers 13:974
21. Lalegani Dezaki M, Mohd Ariffin MKA (2020) The effects of combined infill patterns on mechanical properties in FDM process. Polymers 12:2792
22. Morales MA, Atencio Martinez CL, Maranon A, Hernandez C, Michaud V, Porras A (2021) Development and characterization of rice husk and recycled polypropylene composite filaments for 3D printing. Polymers 13:1067
23. Torres-Alba A, Mercado-Colmenero JM, Caballero-Garcia JDD, Martin-Doñate C (2021) Application of new triple hook-shaped conformal cooling channels for cores and sliders in injection molding to reduce residual stress and warping in complex plastic optical parts. Polymers 13:2944
24. Golmakani ME, Wiczenbach T, Malikan M, Mahoori SM, Eremeyev VA (2021) Experimental and numerical investigation of tensile and flexural behavior of nanoclay wood-plastic composite. Materials 14:2773

Publisher's Note Springer Nature remains neutral with regard to jurisdictional claims in published maps and institutional affiliations.